Title

Quantitative analysis of spatial irregularities in RBCs flows

Authors

Cairone, Fabiana
Mirabella, Daniela
Cabrales, Pedro J
et al.

Publication Date

2018-10-01

DOI

10.1016/j.chaos.2018.07.012

Peer reviewed

Chaos, Solitons and Fractals 115 (2018) 349–355

Contents lists available at ScienceDirect

Chaos, Solitons and Fractals

Nonlinear Science, and Nonequilibrium and Complex Phenomena

journal homepage: www.elsevier.com/locate/chaos

Quantitative analysis of spatial irregularities in RBCs flows

Fabiana Cairone[a,*], Daniela Mirabella[a], Pedro J. Cabrales[b], Marcos Intaglietta[b], Maide Bucolo[a]

[a] Department of Electrical, Electronics and Computer Engineering, University of Catania, viale Andrea Doria 6, Catania 95125, Italy
[b] Department of Bioengineering, University of California San Diego, California, USA

ARTICLE INFO

Article history:
Received 30 April 2018
Revised 13 July 2018
Accepted 13 July 2018
Available online 26 July 2018

Keywords:
Two-phase microfluidics
DPIV analysis
Velocity gradients
Nonlinear indicators

ABSTRACT

The spatial irregularities of red blood cells (RBCs) in continuous pulsing flow condition in micro-channels were investigated by analyzing the time variability of optical signatures obtained by recording transmitted light variability at specific location in micro-flow channels. Different flow conditions were filmed and analyzed by the digital particle image velocimetry (DPIV) to characterize local flow velocity across the whole micro-channel and in four sub-areas selected to study the particles behaviors close to the walls and in the micro-channel bulk. Starting from a behavioral classification based on the three flow patterns identified as {*Weak Activity, Vorticity, Alignment*}, an analysis to detect the spatial irregularity in the flow distribution was carried out. The velocity gradients and four nonlinear parameters (shear rate, strain rate, vorticity, divergence) were computed from the time-varying velocity maps obtained by DPIV and used to provide a quantitative characterization of the flow features. The comparison of the results obtained in the four experiments has made possible an overall understanding of the RBC movements in different conditions and, as well, the establishment of a analysis procedure for flows spatial irregularity detection.

1. Introduction

In the last decade the two-phase microfluidics has contributed in many biological, chemical and medical researches [2,7,19]. The bi-phase flows can be obtained considering two immiscible fluids or micro-particles dispersed in a fluid, with a certain concentration [16].

Real time monitoring of blood flow components is of interest in the field of microvascular research particularly for diagnosing blood pathologies [5,6] and in the development of blood substitutes [1,9]. Blood is composed by plasma and particles and accomplishes its main functions at the micro-vascular level where red blood cells (RBCs) motion evidences the principal dynamic effects due to their preponderant numbers.

A micro-channel network can be then considered the best environment to emulate the RBCs flow in the microvascular system, so the use of microfluidic devices will play a fundamental role in the development of Lab-on-a-chip for blood flows tracking [13–15,17] and blood test [8].

In this context, the establishment of procedures to analyze the RBCs flows, as a standard two-phase microfluidics processes, becomes crucial to study their complex dynamics. In our recent works [3,4], we investigated the collective behavior of the RBCs in micro-channels and three different flow patterns were identified and characterized by the dynamical changes of the particles velocities. To enrich these results, in this paper, the spatial irregularity in RBCs flows in continuous pulsing conditions were studied in the whole micro-channel and in four sub-areas to characterize particles behavior in the bulk micro-channel and close to the walls. The investigation was carried out by using the velocity gradients and four nonlinear parameters (shear rate, strain rate, vorticity, divergence). These nonlinear parameters allowed to describe in details how the particle velocities change in the fluid stream in different experimental conditions, and quantify the spatial features of the flow patterns.

The paper is organized as follows. The Section 2 describes the experimental setup and the digital particle image velocimetry approach used in the RBCs movies analysis. The Section 3 presents the features extracted in the behavioral RBCs flow patterns by using the velocity gradients and the nonlinear parameters in the whole micro-channel and in its sub-areas.

2. Materials and methods

The investigation of the RBCs collective behaviors in a rectilinear micro-channel, in continuous pulsing conditions, was

* Corresponding author.
E-mail addresses: fabiana.cairone@dieei.unict.it, fcairone@dieei.unict.it (F. Cairone).

https://doi.org/10.1016/j.chaos.2018.07.012
0960-0779/

Fig. 1. Experimental setup scheme. The RBCs sample was pumped in the micro-channel by a peristaltic pump (Instech P625). The process was monitored optically by using a backlit white light microscope (BX51, Olympus), with a magnification of 10X and coupled with a high-speed CCD (PCA 1024, Photron).

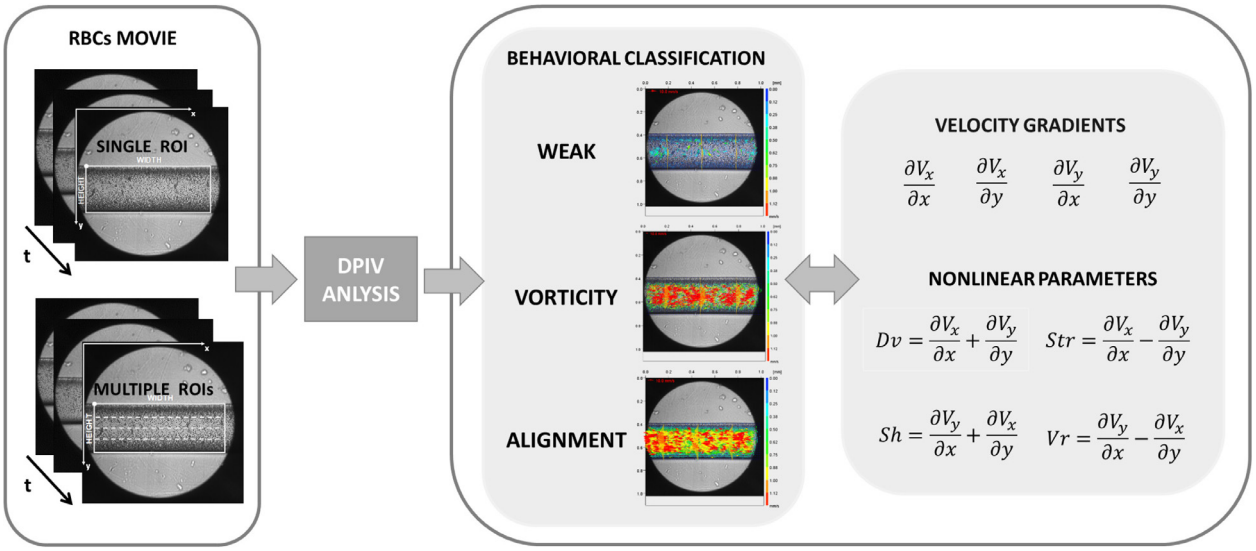

Fig. 2. The flow chart summarizes the key points in this study. The DPIV analysis from the RBCs flow movies performed on the whole micro-channel and in four sub-areas. The investigation based on the velocity gradients and nonlinear parameters to obtain a quantitative characterization of the irregularities in flow pattern behavior.

conducting by using a simplified set-up for process monitoring and the data recording. The movies collected were processed by implementing an automatic procedure based on the digital particle image velocimetry (DPIV) to compute the maps related to the changes in time of the RBCs velocity spatial distributions.

2.1. Experimental setup

RBCs sample was prepared by diluting fresh blood taken from a hamster to a concentration of 1% (hematocrit) in a phosphate buffered saline (PBS) solution. A peristaltic pump (Instech P625) controlled by an ad-hoc LABVIEW interface, was used to feed the fluid in the microfluidic rectilinear channel (SMS0104 ThinxxS), with a squared area of 320 μm^2 side and a length of 16 mm.

Four experiments are presented in which an external oscillating pressure at a frequency $f = 0.1$Hz with an amplitude varying per trial in the set $A \in \{0.1;\ 1;\ 10;\ 100\}$ mmHg was applied at the inlet of the microfluidic channel. The experiments are labelled in the discussion of the results using the values of the forcing amplitude A.

As in the scheme of Fig. 1, the process was optically monitored by a light microscope (*BX*51, Olympus) with a magnification of 10*X* coupled with a high-speed CCD (PCA 1024, Photron). Unlike most of the PIV (particle image velocimetry) analysis, in which the light used is provided by a laser, in this set-up the white light was chosen [11,12] because it is well suited in connection with CCD camera for its spectral sensitivity. Other advantages are the low cost, the simplicity and no needs of particles tracer.

Based on the microscope set-up (Olympus BX51, working distance of the objective 3.5 mm), the focal plane was placed, with a good approximation, at the center of the microchannel. The videos circumscribed an area of 1 mm^2 within the micro-channel at a distance of 8 mm from the inlet. Recording lasted 10 s with a frame rate of 125*FPS* and consist of 1200 frames with a spatial resolution of (1024×1024) px, based on the optical setup used 1 px $= 1\,\mu$m.

2.2. DPIV analysis

The RBCs movies acquired were analyzed by using the digital particle image velocimetry (DPIV) [12], the output information investigated were the time-varying velocities vector maps. The analysis was carried out in the portion of the frame occupied by the micro-channel, called region of interest (ROI), whose width and height are respectively {1000, 300} px.

In the DPIV algorithm, the analysis was performed by implementing the cross-correlation between interrogation areas of two consecutive images. Specifically, the approach used was the discrete Fourier transform (DFT), that computes the correlation matrix in the frequency domain. In this work, a three-pass DFT was considered, where the three squared subsequent interrogation areas in pixel were chosen as follows: $InterrArea1 = 64$, $InterrArea2 = 32$, $InterrArea3 = 16$. The step size has been set a half of the last interrogation area, $Step = 8$. In this way, the smallest displacement investigated was of about 8 µm, close to the RBC dimension.

In [3], the analysis of the RBCs movies to compute the velocity vector maps $V(i, j, t)$ was conducted using the JPIV platform [20]. Instead in this work, the PIVlab tool for Matlab [18] was used. This gives, as output information, the matrices related to the spatial distribution of the velocity components on the horizontal and vertical directions $\{V_x(i, j, t), V_y(i, j, t)\}$.

The accuracy of the measure was taken into account using an experiment where a single-phase PBS solution was fed at the inlet

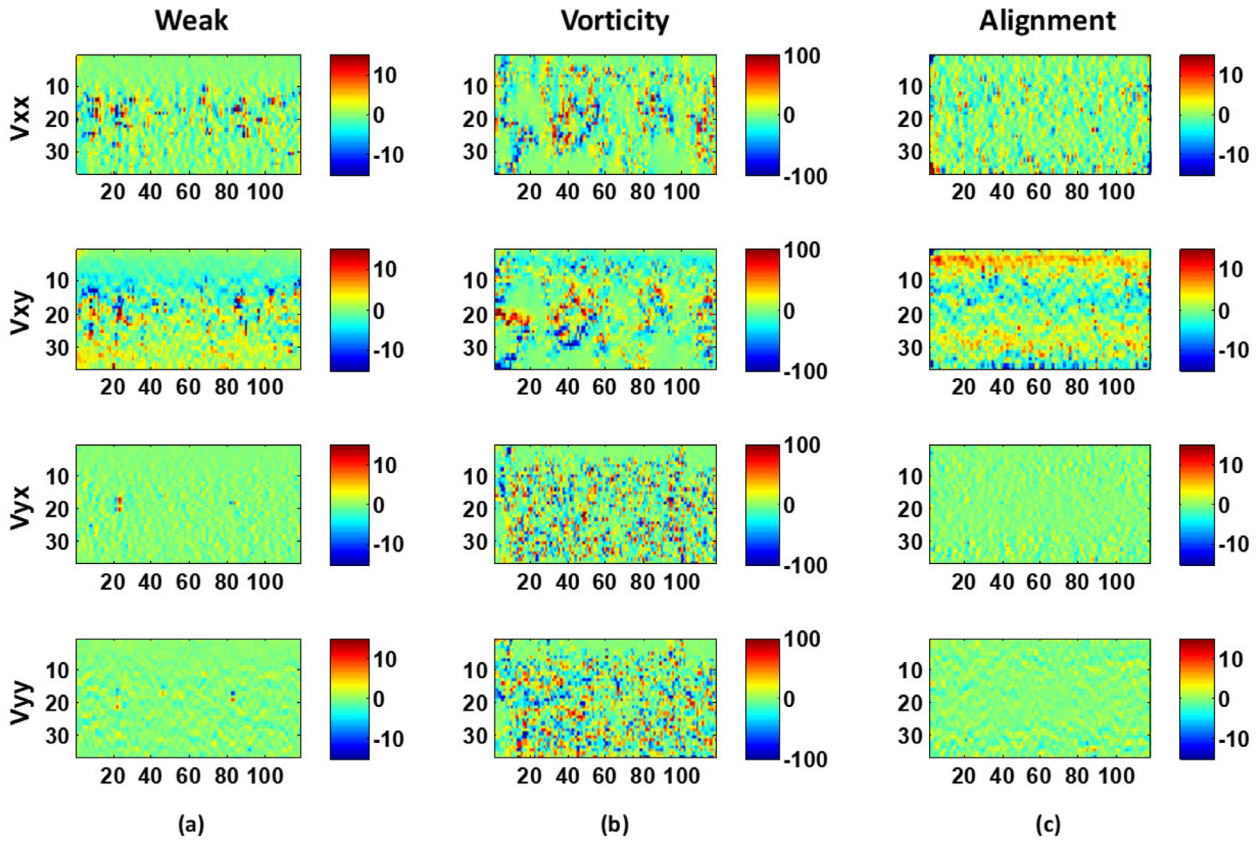

Fig. 3. The standard distribution of the four RBCs velocity gradients in a time instant t^*. The behavior {*Weak Activity, Vorticity, Alignment*} are arranged in columns. The velocity gradients are arranged in rows $\{V_{xx}(i, j, t^*), V_{xy}(i, j, t^*), V_{yx}(i, j, t^*), V_{yy}(i, j, t^*)\}$.

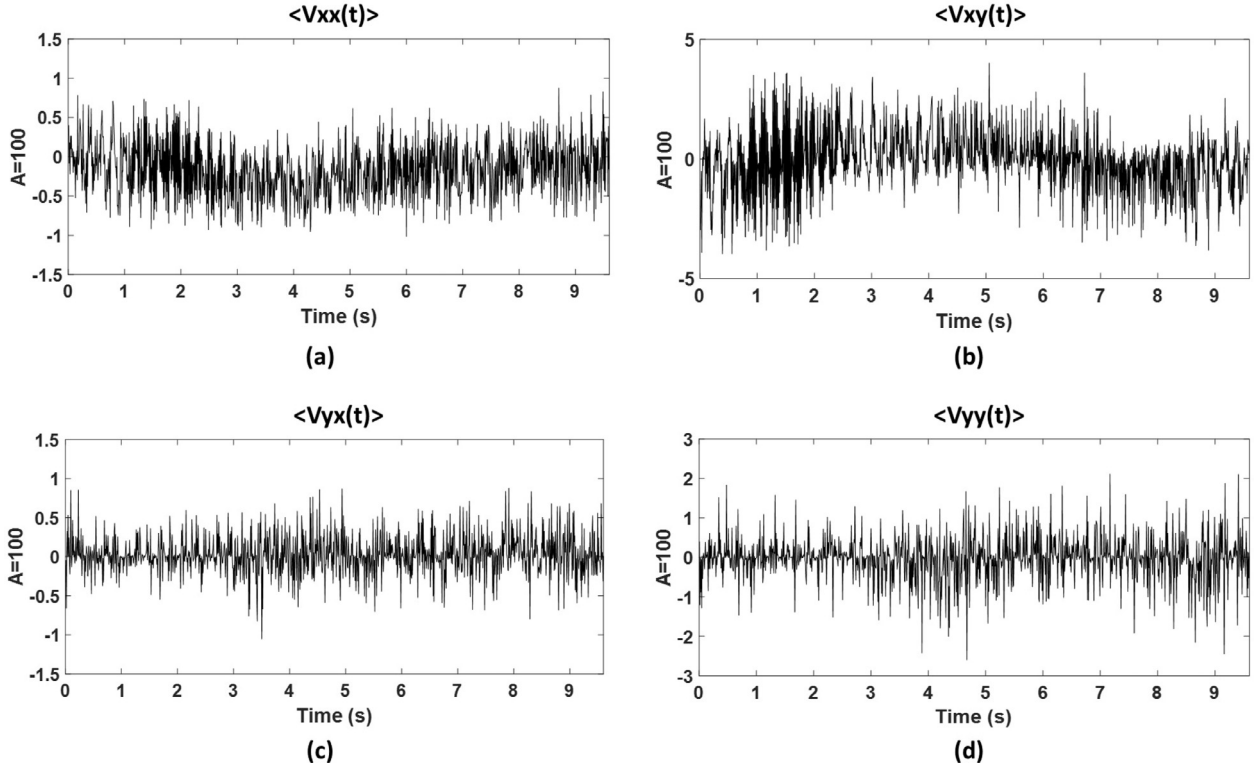

Fig. 4. In the experiment $A = 100$, the signals $\{ < V_{xx}(t) >, < V_{xy}(t) >, < V_{yx}(t) >, < V_{yy}(t) > \}$ related to the average in the micro-channel area of the gradient maps.

of the micro-channel with an oscillating pressure with a frequency $f = 0.1$ Hz and an amplitude of $A = 100$ mmHg. Then the movie acquired was analyzed and the velocity obtained used as reference value to quantify of the background noise respect to the cases in which the RBCs displacements were detected [3].

3. Spatial nonlinearity in RBCs flows

In [3], examining the velocity vector maps, the RBCs movements were classified in three behavioral flow patterns: *Weak Activity, Vorticity* and *Alignment*. The *Weak Activity* was associated with a powerless and localized random stream. The *Vorticity* was related of the RBCs displacements in vortex randomly distributed along the channel length caused by the velocity vectors re-orientation. The *Alignment* was defined as an ordered arrangement of RBCs along the horizontal direction. The spatial distribution of the RBCs velocity in the micro-channel was investigated by using the velocity gradients and some related nonlinear parameters. The analysis was carried out in the whole micro-channel (ROI) and by splitting that in four smaller areas. The flow chart in Fig. 2 summarizes the key points in this study.

3.1. Analysis by velocity gradients

Being the flows highly complex, some conditions are hardly classified by the velocity maps. To overcome those limitations attention was focused on the RBCs spatial distributions in the ROI by using the gradients of the velocities on the horizontal and vertical directions ($V_x(i, j, t)$ and $V_y(i, j, t)$). These gradients, describing the particles velocity spread on the fluid stream, were calculated as follows:

$$V_{xx}(i, j, t) = \frac{\partial V_x(i, j, t)}{\partial x} \tag{1}$$

$$V_{xy}(i, j, t) = \frac{\partial V_x(i, j, t)}{\partial y} \tag{2}$$

$$V_{yx}(i, j, t) = \frac{\partial V_y(i, j, t)}{\partial x} \tag{3}$$

$$V_{yy}(i, j, t) = \frac{\partial V_y(i, j, t)}{\partial y} \tag{4}$$

where (i, j) represent the $2D$ coordinates of a generic point in the velocity and gradient maps, that are associated respectively to the particles displacement on the horizontal (x) and the vertical (y) directions. The variable t expresses the map variability over time. Fig. 3 shows the standard distribution of the four RBCs velocity gradients $\{V_{xx}(i, j, t^*), V_{xy}(i, j, t^*), V_{yx}(i, j, t^*), V_{yy}(i, j, t^*)\}$ in a time instant t^* (arranged in rows) per behavior {*Weak Activity, Vorticity, Alignment*} (arranged in columns). The dimension of the velocity maps on the x and y axes are (124×36) px, obtained by the DPIV analysis in relation to the ROI size, the values of the interrogation areas and the quantization step [3]. Each image is plotted using a color-code to evidence those areas where RBCs velocity changes mostly. Those variations are one order higher in the case of *Vorticity* than for the *Weak Activity* and *Alignment*. Additionally it is worth to notice that no activity was detected in the gradients $\{V_{yx}(i, j, t^*), V_{yy}(i, j, t^*)\}$ for the *Weak Activity* and *Alignment*, whereas random variations are in *Vorticity*. The gradients $\{V_{xx}(i, j, t^*), V_{xy}(i, j, t^*)\}$ are more active in the bulk channel for the *Weak Activity* and, arranged in streamlines for the *Alignment* and in zones for the *Vorticity*.

To focus the attention on the changes over time of the four velocity gradients, their averages in the investigated area $\{ < V_{xx}(t) >, < V_{xy}(t) >, < V_{yx}(t) >, < V_{yy}(t) > \}$ were considered.

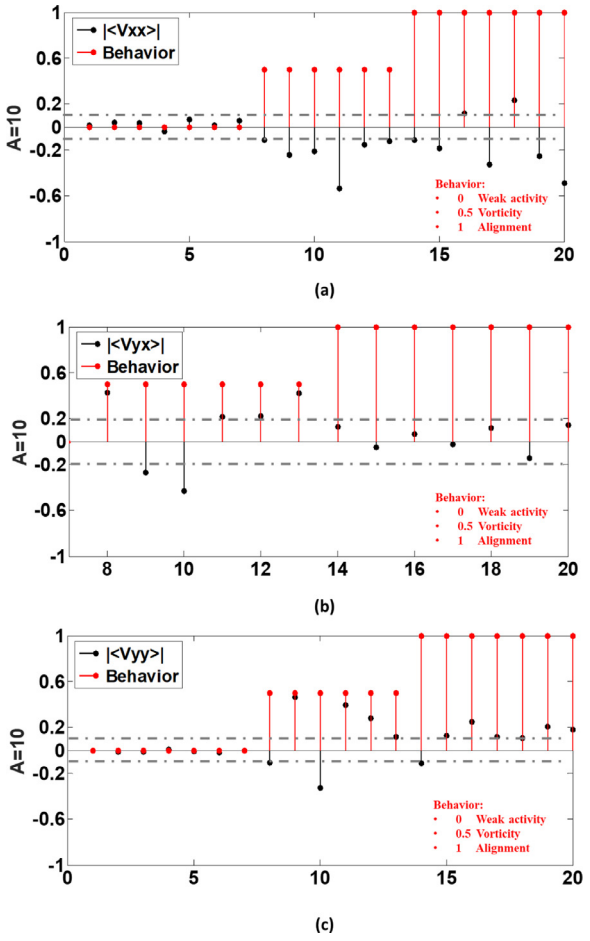

Fig. 5. Association between the RBCs behavior in the 20 frames selected with the mean of each velocity gradients for the experiment $A = 10$. The three stem diagrams are for (a) $|< V_{xx} >|$, (b) $|< V_{yx} >|$, (c) $|< V_{yy} >|$. The black-stems are for the absolute value of mean velocity gradient samples and the red-stems are for the behavioral coding. (For interpretation of the references to color in this figure legend, the reader is referred to the web version of this article.)

In Fig. 4, the signals related of the average of the gradient maps for the experiment $A = 100$ are plotted. Both gradient mean variations of $\{ < V_{xx}(t) >, < V_{xy}(t) >$ (see Fig. 4(a)–(b)) are affected by the pump activity, showing a periodic oscillation at 0.1 Hz similarly to the $< V_x(t) >$ trend in [3]. This is a very apparent effect in $< V_{xy}(t) >$. To point on the RBCs irregular behaviors, this parameter was neglected, and only the gradient mean variations related to $\{ < V_{xx}(t) >, < V_{yy}(t) >, < V_{yx}(t) > \}$ were used in the further analysis.

20 frames of the velocity vector maps [3] were randomly extracted for each experiment $A \in \{0.1, 1, 10, 100\}$.

Those frames were classified based on the RBCs behavior {*Weak Activity, Vorticity* and *Alignment*} respectively using the coding system {0, 0.5, 1}, and then paired with the correlated samples of the velocity gradients signals (labeled $\{ < V_{xx} >, < V_{yx} >, < V_{yy} > \}$). In Figs. 5 and 6, respectively, for the experiments $A \in \{10, 100\}$, the RBCs behaviors per frame were associated with the values of mean of each velocity gradients using stem diagrams. The black-stems are for the absolute value of mean velocity gradient samples $\{|< V_{xx} >|, |< V_{yx} >|, |< V_{yy} >|\}$ (see sub-figure (a),(b),(c), respectively) and the red-stems are for the behavioral code.

By these plots it was evident the possibility to establish a classification criteria in two steps. In the first step, the values of the gradients $\{|< V_{xx} >|, |< V_{yy}(t) >|\}$ were used to have information about the presence of a significant RBCs activity in the flow to dis-

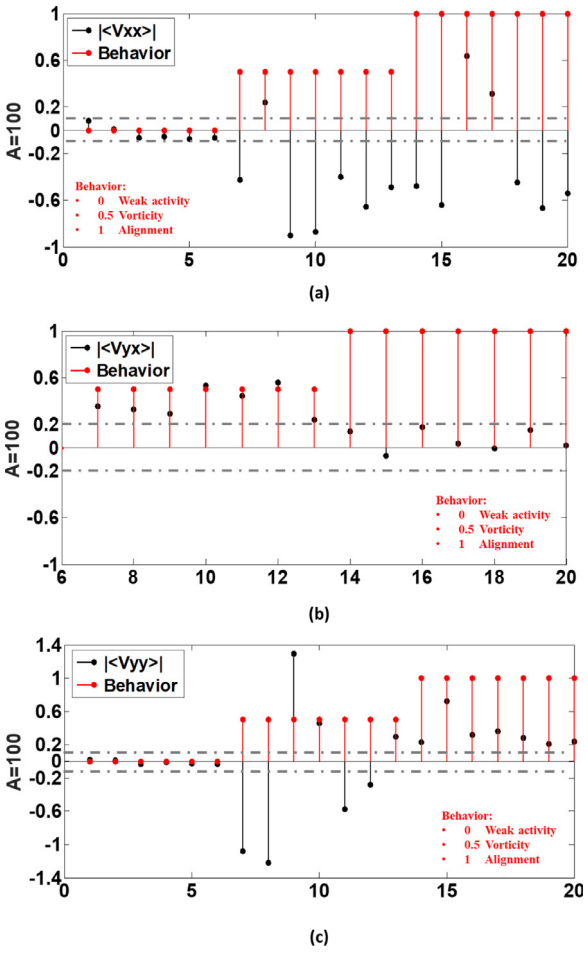

Fig. 6. Association between the RBCs behavior in the 20 frames selected with the mean of each velocity gradients for the experiment $A = 100$. The three stem diagrams are for (a) $|<V_{xx}>|$, (b) $|<V_{yx}>|$, (c) $|<V_{yy}>|$. The black-stems are for the absolute value of mean velocity gradient samples and the red-stems are for the behavioral coding. (For interpretation of the references to color in this figure legend, the reader is referred to the web version of this article.)

tinguish the *Weak Activity* from the *Strong Activity* including {*Vorticity* and *Alignment*}. Particularly the threshold thr_1 was defined per experiment $A \in \{10, 100\}$ respectively equal to $thr_1 = \{0.1, 0.2\}$, the classification rule follows:

- *Weak Activity* is for $|V_{xx}| \le thr_1$ or $|V_{yy}| \le thr_1$;
- *Strong Activity* is for $|V_{xx}| > thr_1$ or $|V_{yy}| > thr_1$.

A greater threshold for $A = 100$ was required, because the increase of the pump strength induced higher velocities in the RBCs flow. In the second step, the values of the gradient V_{yx} were used to distinguish between *Vorticity* and *Alignment*. The same threshold value thr_2 was set for both experiments $A = \{10, 100\}$ respectively equal to $thr_2 = 0.2$, the classification rule follows:

- *Alignment* is for $|V_{yx}| \le thr_2$;
- *Vorticity* is for $|V_{yx}| > thr_2$.

3.2. Nonlinear analysis in the whole micro-channel

To examine in depth the irregularity in the RBCs flows a further investigation based on a set of nonlinear parameters were carried out: the divergence (*Dv*), the shear rate (*Shr*), the strain rate (*Str*) and the vorticity (*Vr*) [10]. The time-varying maps of those parameters were obtained as combinations of the velocity gradients maps as follows in Eqs. (5)–(8).

$$Dv(i, j, t) = V_{xx}(i, j, t) + V_{yy}(i, j, t) \tag{5}$$

$$Shr(i, j, t) = V_{yx}(i, j, t) + V_{xy}(i, j, t) \tag{6}$$

$$Str(i, j, t) = V_{xx}(i, j, t) - V_{yy}(i, j, t) \tag{7}$$

$$Vr(i, j, t) = V_{yx}(i, j, t) - V_{xy}(i, j, t) \tag{8}$$

As in the case of the velocity gradients, those parameters were averaged in the investigated area and the four signals obtained $\{<Dv(t)>, <Shr(t)>, <Str(t)>, <Vr(t)>\}$ are plotted for the experiment $A\{100\}$ in Fig. 7. It can be noticed that the shear rate (Fig. 7(b)) and the vorticity (Fig. 7(d)) are affected by the pumps activity being both related to $V_{xy}(i, j, t)$ with opposite sign. Fig. 8 shows the statistical distributions of those parameters (in absolute value) for each experiment $A \in \{0.1, 1, 10, 100\}$. Fig. 8(a) is for $|<Dv(t)>|$ and $|<Str(t)>|$, whereas Fig. 8(b) for $|<Vr(t)>|$ and $|<Shr(t)>|$. Due to the overlap of their statistical distributions in pair, the statistics in the following analysis were computed using the two parameters $|<Dv(t)>|$ and $|<Vr(t)>|$. Particularly, the mean value of the signals $|<Dv(t)>|$ and $|<Vr(t)>|$, labeled respectively μ_{dv} and μ_{vr} were computed per experiment and plotted in the bar diagram of Fig. 9. In the previous work [3], the *Vorticity* is mostly present in the experimental conditions $A \in \{10, 100\}$, whereas the *Alignment* in $A = 100$. In Fig. 9(a) the values of μ_{dv} are almost equal for $A \in \{0.1, 1, 10\}$ and suddenly increases in $A = 100$, showing the same variation discussed for $<|Vx(t)|>$ in the paper [3]. That confirms the possibility to detect by the parameter divergence the RBCs *Alignment* in the flow. This is strongly correlated with velocity values and gradients along the horizontal direction x pressure-driven by the pump. In Fig. 9(b) considering μ_{vr} two levels can be distinguished: a lower for $A \in \{0.1, 1\}$ and a greater for $A \in \{10, 100\}$. Consequently the parameters vorticity in both those experiments can be used to enhance the *Vorticity* behavior in which the RBCs velocity values and gradients in both x, y directions are high but neither prevails over the other. In the bar plot of μ_{vr} it is interesting to notice a higher value corresponding to experiment $A\{10\}$ than in $A\{100\}$, caused by a balanced presence in the latter case of both *Vorticity* and *Alignment* patterns.

3.3. Nonlinear analysis in micro-channel sub-areas

The potentiality of the nonlinear parameters becomes more evident in the RBCs flow investigation reducing the dimension of regions of interest. The whole region of interest (as indicated in the Section 3.2) was divided in four sub-regions. Leaving the width dimension unchanged, the ROI height (300 pixel) was split in a way to have the height of two areas near to the channel boundaries half of the two central areas respectively 50 px and 100 px. The aim was to capture distinctions in the flow profiles related to the RBCs behaviors close to the channel boundaries and in the bulk micro-channel. The same analysis procedure presented in Section 3.2 was carried out, and the two parameters (μ_{dv}, μ_{vr}) for all the experiments and the four sub-areas were computed and plotted in Fig. 10. In both bar diagrams of (μ_{dv}, μ_{vr}) for the experiments $A \in \{0.1, 1, 10\}$ the values of the parameters are greater in the central sub-regions than in those external. The asymmetry of their profiles is due to particles random distribution. Conversely in the experiment $A = 100$ the values are greater in the external subregions, especially in the parameter μ_{vr}. This change is due to the flow regularization induced by the RBCs alignment in the bulk channel. The flow closed to the channel boundary become more irregular due to the RBCs collisions with the channel walls and

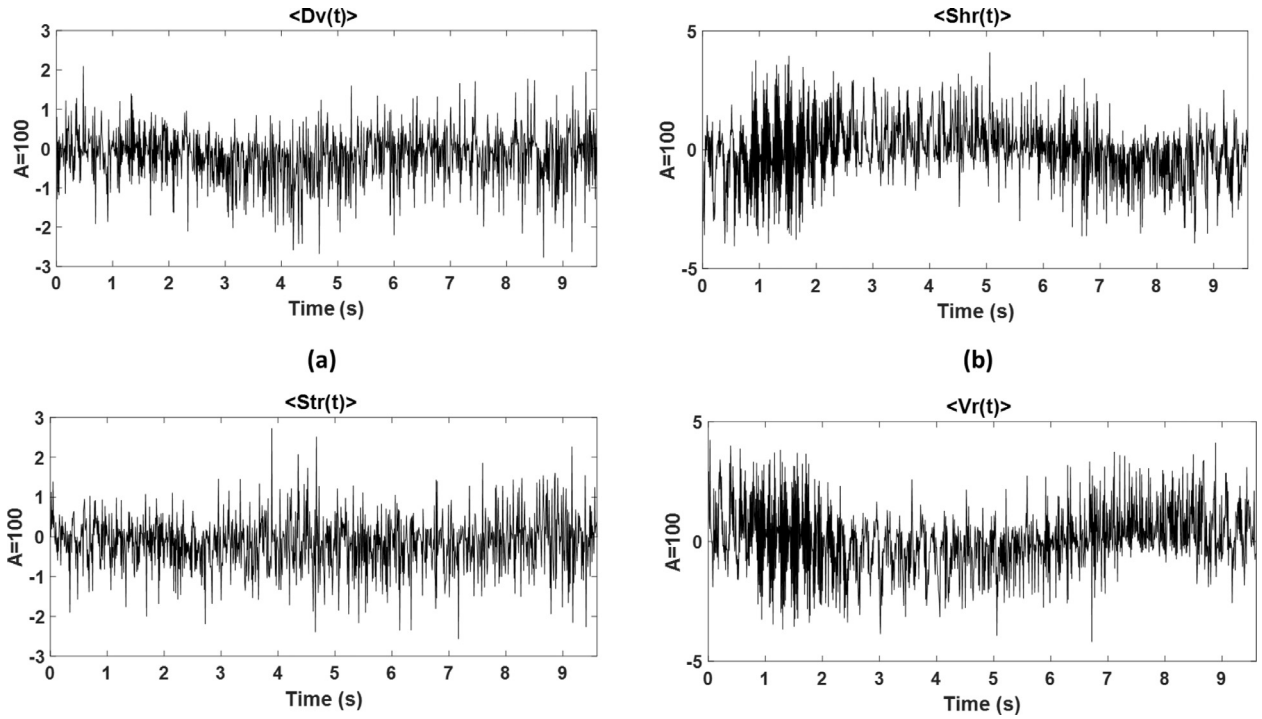

Fig. 7. The trends of the four signals $\{<Dv(t)>, <Shr(t)>, <Str(t)>, <Vr(t)>\}$ obtained by averaging in the investigation area the time-varying maps of the nonlinear parameters: (a) the divergence (*Dv*), (b) the shear rate (*Shr*), (c) the strain rate (*Str*) and (d) the vorticity (*Vr*).

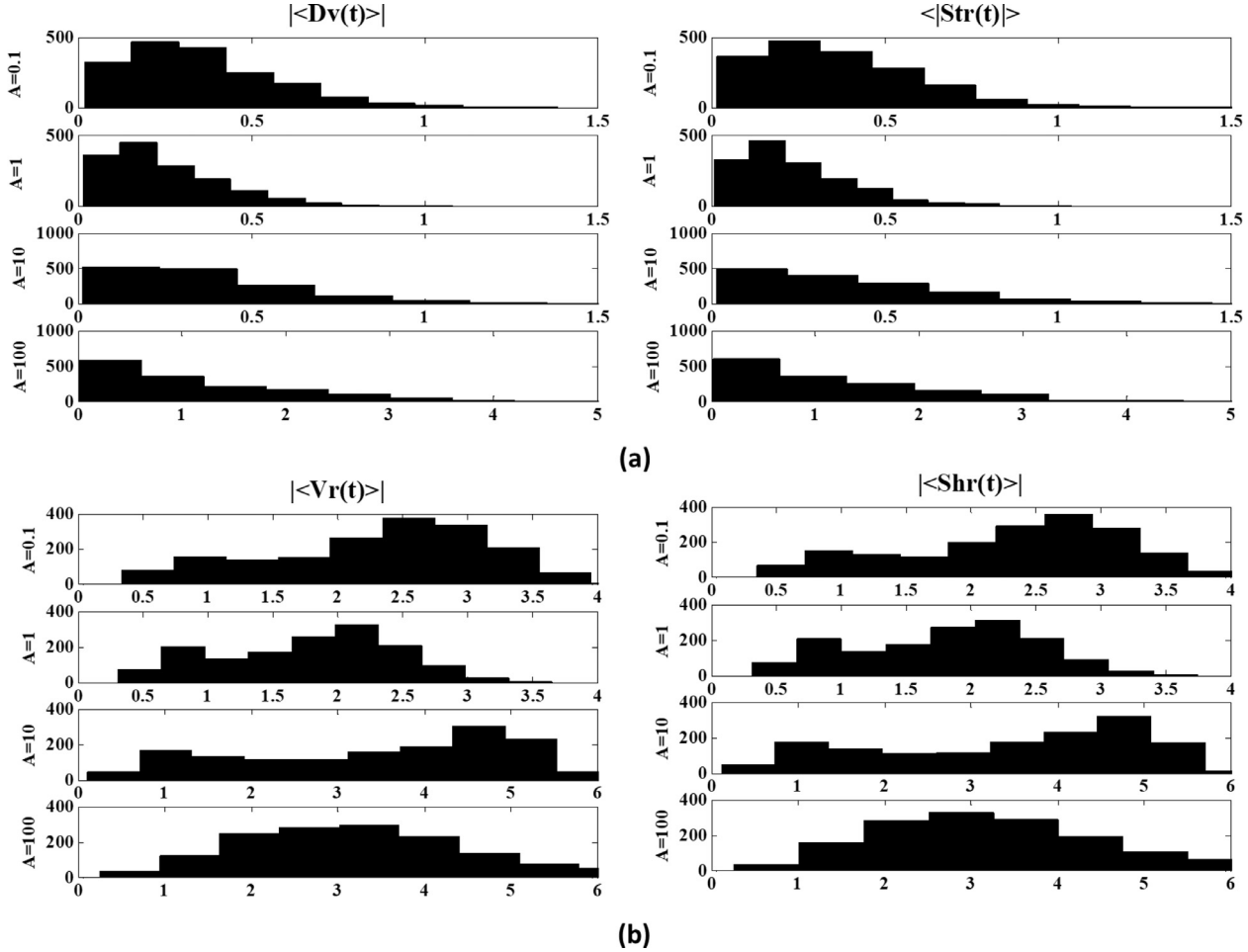

Fig. 8. Statistical distributions of (a) $|<Dv(t)>|$ and $|<Str(t)>|$, (b) $|<Vr(t)>|$ and $|<Shr(t)>|$ for all the experiments $A \in \{0.1, 1, 10, 100\}$.

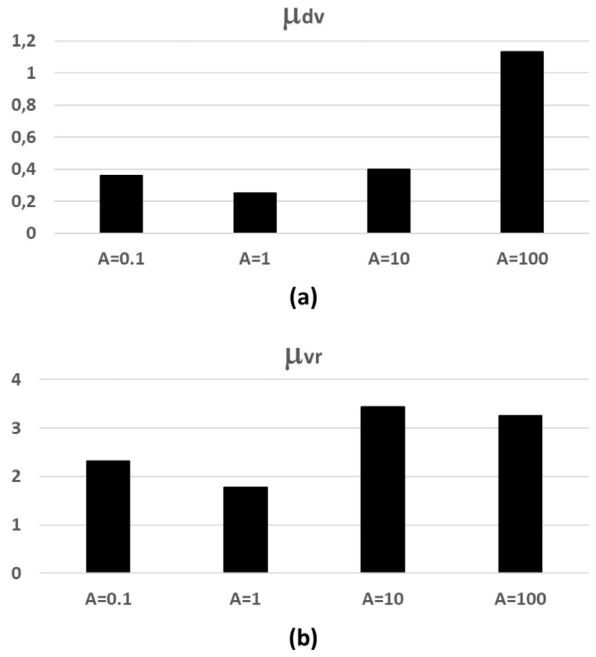

Fig. 9. The bar diagrams for the analysis in the whole micro-channel (ROI) of (a) the mean value of the $|<Dv(t)>|$ signal μ_{dv} and (b) the mean value of the $|<Vr(t)>|$ signal μ_{vr}, for all the experiments $A \in \{0.1, 1, 10, 100\}$.

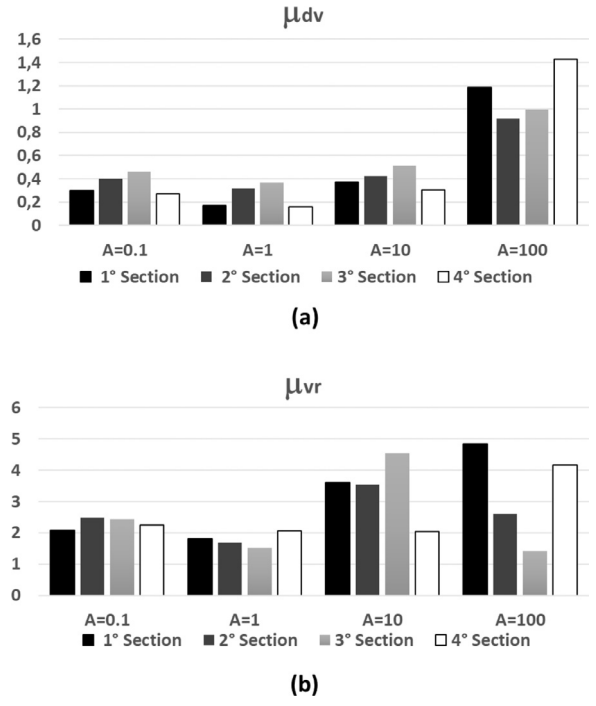

Fig. 10. The bar diagrams for the analysis in multiple-areas of (a) the mean value of the $|<Dv(t)>|$ signal μ_{dv} and (b) the mean value of the $|<Vr(t)>|$ signal μ_{vr}, for all the experiments $A \in \{0.1, 1, 10, 100\}$.

the simultaneous action of the pressure-drive strength and viscous force. The sensitivity of the parameter μ_{vr} to the irregular RBCs behavior is also highlighted by the profile of the bar plot in the experiment $A = 10$, where the irregular behavior in the bulk micro-channel equals that at the boundary.

4. Conclusions

The paper investigates spatial irregularity in RBCs flows in a micro-channel in continuous pulsing conditions. The DPIV analysis of four RBCs flows movies was performed considering as region of interest the whole micro-channel and four sub-areas, to characterize the particles behaviors in the bulk micro-channel and close to the walls. The investigation was carried out by using the velocity gradients and four nonlinear parameters (shear rate, strain rate, vorticity, divergence). By these parameters, the quantitative characterization of the irregularities in three behavioral flow patterns {*Weak Activity, Vorticity, Alignment*} identified in [3] was obtained. The comparison of the results in the four experimental conditions was used for the overall understanding of the RBC movements in different conditions and to generalize the analysis procedure.

The establishment of an automatic procedure for the quantitative analysis of the flow features has been one of the focal points of the study. The investigation of RBC flows in a wider experimental study will be considered as a future development of this work to verify and generalize the obtained results. The use of the developed procedure to monitor the RBCs flow in microfluidics devices with irregular micro-channel geometries will permit the determination of fluid flow resistances within microchannel as well as the quantification of the high fluid shear forces sustained on blood components in complex flows.

References

[1] Bowersox JC, Hess JR. Trauma and military applications of blood substitutes. Int J Artif Cells Blood Substitutes Immobilization Biotechnol 1994;22(2):145159.
[2] Bucolo M, Guo J, Intaglietta M, Coltro W. Guest editorial, special issue on microfluidics engineering for point-of-care diagnostics. IEEE Trans Biomed Circuits Syst 2017;11(6):1488–99.
[3] Cairone F, Ortiz D, Cabrales PJ, Intaglietta M, Bucolo M. Emergent behaviors in RBCs flows in micro-channels using digital particle image velocimetry. Microvasc Res 2018;116:77–86.
[4] Cairone F, Sanalitro D, Ortiz D, Cabrales PJ, Intaglietta M, Bucolo M. DPIV analysis of RBCs flows in serpentine micro-channel. European conf. on circuit theory and design (ECCTD); 2017. Catania, Italy, September 4–6, 2017
[5] Cakmak G, Alkan FA, Korkmaz K, Saglam ZA, Karis D, Yenigun M, Ercan M. Blood viscosity as a forgotten factor and its effect on pulmonary flow. Trans Respir Med 2013;1(3):1–5.
[6] Dintenfass L. Blood rheology in pathogenesis of the coronary heart diseases. Am Heart J 1969;77:139–47.
[7] Janasek D, Franzke J, Manz A. Scaling the design of miniaturized chemical analysis system. Nature 2006;42:374380.
[8] Kang YJ, Yeom E, Lee SJ. A microfluidic device for simultaneous measurement of viscosity and flow rate of blood in a complex fluidic network. Biomicrofluidics 2013;7:054111.
[9] Klein HG. Oxygen carriers and transfusion medicine. Int J Artif Cells Blood Substitutes Immobilization Biotechnol 1994;22(2):123135.
[10] Majda AJ, Bertozzi AL. Vorticity and incompressible flow. Cambridge University Press; 2002.
[11] Poelma C, Kloosterman A, Hierck BP, Westerweel J. Accurate blood flow measurements: are artificial tracers necessary? PLoS ONE 2 2012;7(9):e45247.
[12] Raffel M, Willert CE, Wereley S, Kompenhans J. Particle image velocimetry: a practical guide. Springer; 1998.
[13] Sapuppo F, Bucolo M, Intaglietta M, Fortuna L, Arena P. Cellular non-linear networks for microcirculation applications. Int J Circuit Theory Appl 2006;34(4):471:488.
[14] Sapuppo F, Bucolo M, Intaglietta M, Johnson PC, Fortuna L, Arena P. An improved instrument for real-time measurement of blood velocity in microvessels. Trans on Instrum Meas 2007;56(6):2663–71.
[15] Sapuppo F, Intaglietta M, Bucolo M. Microfluidics real-time monitoring using CNN technology. IEEE Trans Biomed Circuits Syst 2008;2(2):78:87.
[16] Sapuppo F, Schembri F, Fortuna L, Bucolo M. Microfluidics circuits and systems. IEEE Circuit Syst Mag 2009;9(3):6:19. Third Quarter
[17] Sapuppo F, Llobera A, Schembri F, Intaglietta M, Cadarso VJ, Bucolo M. A polymeric micro-optical interface for flow monitoring in bio-microfluidics. Biomicrofluidics 2012;4(1):1–13.
[18] Thielicke W, Stamhuis EJ. PIVlab towards user-friendly, affordable and accurate digital particle image velocimetry in MATLAB. J Open Res Software 2014;2. E30
[19] Whitesides GM. The origins and the future of microfluidics. Nature 2006;442:368–73.
[20] http://www.jpiv.vennemann-online.de/.